Supporting Information

Confining gold nanoparticles in preformed zeolites by post-synthetic modification enhances stability and catalytic reactivity and selectivity

Eunji Eom,[a] Minseok Song,[a] Jeong-Chul Kim,[b] Dong-il Kwon,[a] Daniel N. Rainer,[c] Kinga Gołąbek,[c] Sung Chan Nam,[d] Ryong Ryoo,[e] Michal Mazur,[c,*] and Changbum Jo[a,*]

[a]Department of Chemistry and Chemical Engineering, Inha University, 100 Inha-ro, Michuhol-gu, Incheon, 22212, Republic of Korea

[b]Center for Nanomaterials and Chemical Reactions, Institute for Basic Science (IBS), Daejeon 34141, Republic of Korea

[c]Department of Physical and Macromolecular Chemistry, Faculty of Science, Charles University, Hlavova 8, 128 43 Prague, Czech Republic

[d]Greenhouse Gas Research Laboratory, Korea Institute of Energy Research, Daejeon 34129, Republic of Korea

[e]KENTECH Laboratory for Chemical, Environmental and Climate Technology Korea Institute of Energy Technology (KENTECH) 200 Hyeoksin-ro, Naju 58330, Republic of Korea

[*]Corresponding Authors

Email: michal.mazur@natur.cuni.cz (M.M.); jochangbum@inha.ac.kr (C.J.)

Calculation method of the fraction of edge and corner sites of nanoparticles.

We assumed that Au nanoparticles have truncated octahedron geometry (see below figure). The fraction of edge and corner sites was calculated according to the previous paper reported elsewhere (*Chem. Eng. J.* 2021, *425*, 130642; *J. Nanopart. Res.* 2016, *18*, 295).

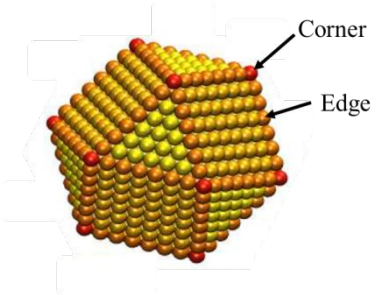

(1) Number of metal atoms at corner sites (N_{corner}): 24

(2) Number of metal atoms at edge sites (N_{edge}): $36 \times (m-2)$, where m means the number of atoms lying on an equivalent edge, which is related to the cluster diameter through $d_{cluster} = m \times 2d_{at}$ (d_{at} = van der Waals diameter)

(3) Total number of atoms in metal clusters (N_T): $16 \times m^3 - 33 \times m^2 + 24 \times m - 6$

Fraction of corner sites: N_{corner}/N_T

Fraction of edge sites: N_{edge}/N_T

Table S1. Fitting results for the series of *x*Au/f-beta and *x*Au/f-MFI samples

	N_{Au-Au}	R_{Au-Au} (Å)	Debye-waller factor (σ^2)	ΔE_0 (eV)	R-factor
Au foil	12	2.86	0.00794	4.28	0.00150
1.3 Au/f-beta	10.7	2.85	0.00808	4.43	0.0319
0.48 Au/f-beta	10.3	2.85	0.00863	3.00	0.041
0.28 Au/f-beta	9.58	2.85	0.00814	4.60	0.00684
1.1 Au/u-beta	11.4	2.86	0.00790	4.13	0.00236
0.48 Au/f-MFI	10.1	2.85	0.00827	4.40	0.00606
0.28 Au/f-MFI	8.42	2.84	0.00732	2.25	0.0211
0.18 Au/f-MFI	-	-	-	-	-
0.48 Au/u-MFI	11.8	2.86	0.00578	3.23	0.00578

Table S2. Summary of catalytic performance for CO oxidation under humid conditions over supported Au catalysts

Catalysts	Reaction conditions	Temperature (°C)	Converted CO/Au [(mol/min)/mol]	Ref
1.3wt% Au/f-beta	0.10g, 0.5% CO, 10% O_2 and 5.0% H_2O balanced with Ar, total flow 16.5 ml/min	40	0.016	-
0.48wt% Au/f-beta			0.042	
0.28wt% Au/f-beta			0.056	
0.48wt% Au/f-MFI			0.053	
0.28wt% Au/f-MFI			0.13	
0.18wt% Au/f-MFI			0.29	
1.9wt% Au/MOR	0.10g, 1% CO and 1% O_2 balanced with He, total flow 40 ml/min	40	0.11	1
2.9wt% Au/SiO_2	0.050g, 1% CO and 0.5% O_2 balanced with He, total flow 40 ml/min	40	0.61	2
1.7wt% Au/Y	0.035g, 1% CO and 99% Air, total flow 33 ml/min	40	4.8	3
5.0wt% Au@ZIF-8	0.10g, 1% CO and 21% O_2 balanced with He, total flow 100 ml/min	40	0.048	4
1.3wt% Au/ZnO	0.50g, 0.5% CO, 10% O_2 and 1.8% H_2O balanced with Ar, total flow rate 100 ml/min	25	0.079	5
1.0% Au-TiO2(I)	0.050g, 4.9% CO, 4.9% O_2 and 0.59% H_2O balanced with He, total flow 35 ml/min	40	0.00063	6
0.37wt% Au/CeO_2 /Al_2O_3	0.080g, 5% CO, 5% O_2 and balanced with He	40	11	7

	total flow 84 ml/min			
1.4wt% Au/$CaCO_3$	0.50g, 0.5% CO, 10% O_2 and 1.8% H_2O balanced with Ar, total flow rate 100 ml/min	70	0.12	8
5.0wt% Au/Co_3O_4	0.10g, 2.0% CO (bal. He), 1.25% H_2O mixing with high purity air (99.999%), total flow 50 ml/min	40	0.013	9

Reference

1. Simakov, A.; Tuzovskaya, I.; Pestryakov, A.; Bogdanchikova, N.; Gurin, V.; Avalos, M.; Farías, M., On the nature of active gold species in zeolites in CO oxidation. *Appl. Catal. A-Gen.* 2007, *331,* 121-128.
2. Bogdanchikova, N.; Pestryakov, A.; Tuzovskaya, I.; Zepeda, T.; Farias, M.; Tiznado, H.; Martynyuk, O., Effect of redox treatments on activation and deactivation of gold nanospecies supported on mesoporous silica in CO oxidation. *Fuel* 2013, *110*, 40-47.
3. Lin, J.-N.; Chen, J.-H.; Hsiao, C.-Y.; Kang, Y.-M.; Wan, B.-Z., Gold supported on surface acidity modified Y-type and iron/Y-type zeolite for CO oxidation. *Appl. Catal. B.* 2002, *36* (1), 19-29.
4. Jiang, H.-L.; Liu, B.; Akita, T.; Haruta, M.; Sakurai, H.; Xu, Q., Au@ ZIF-8: CO oxidation over gold nanoparticles deposited to metal− organic framework. *J. Am. Chem. Soc.* 2009, *131* (32), 11302-11303.
5. Wang, G. Y.; Zhang, W. X.; Lian, H. L.; Wu, T. H., Effect of calcination temperatures and precipitant on the catalytic performance of Au/ZnO catalysts for CO oxidation at ambient temperature and in humid circumstances. *Appl. Catal. A-Gen.* 2003, *239* (1-2), 1-10.
6. Bollinger, M. A.; Vannice, M. A., A kinetic and DRIFTS study of low-temperature carbon monoxide oxidation over Au—TiO_2 catalysts. *Appl. Catal. B.* 1996, *8* (4), 417-443.
7. Centeno, M. Á.; Portales, C.; Carrizosa, I.; Odriozola, J. A., Gold supported CeO_2/Al_2O_3 catalysts for CO oxidation: influence of the ceria phase. *Catal. Lett.* 2005, *102* (3), 289-297.
8. Lian, H.; Jia, M.; Pan, W.; Li, Y.; Zhang, W.; Jiang, D., Gold-base catalysts supported on carbonate for low-temperature CO oxidation. *Catal. Commun.* 2005, *6* (1), 47-51.
9. Kim, K.-J.; Chung, M.-C.; Ahn, H.-G., Effect of Water Addition on Catalytic Activity of Nanosized Gold Catalysts for CO Oxidation. *J. Nanosci. Nanotechnol.* 2011, *11* (8), 7471-7474.

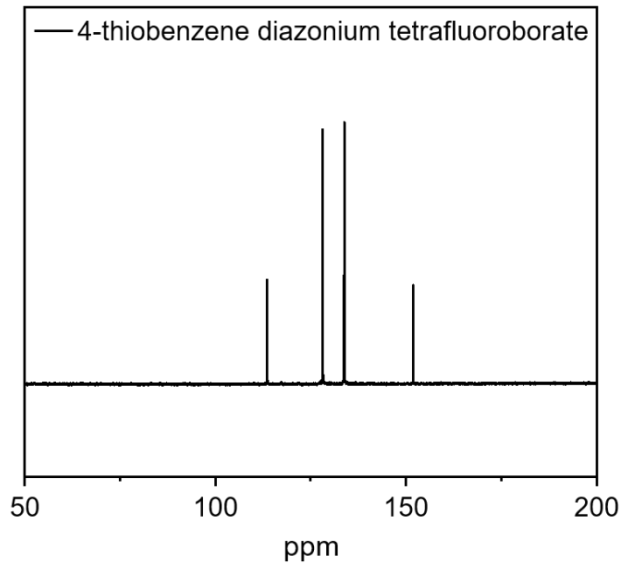

Figure S1. ^{13}C NMR spectrum of 4-thiobenzene diazonium tetrafluoroborate

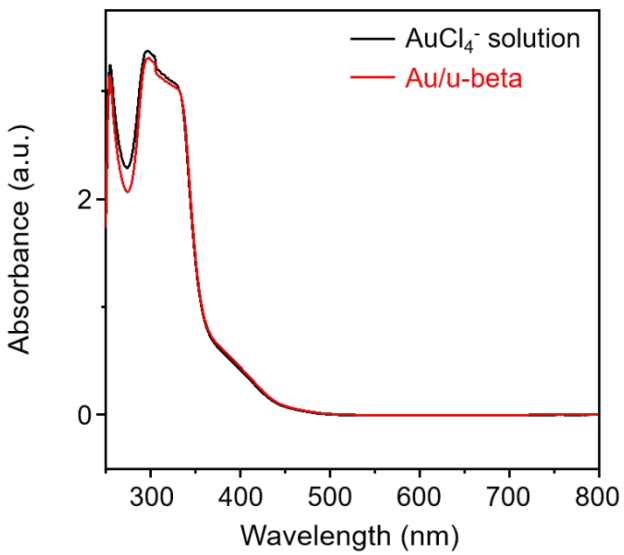

Figure S2. UV-visible spectra of the pure $AuCl_4^-$ solution and filtrate of the Au/u-beta solution

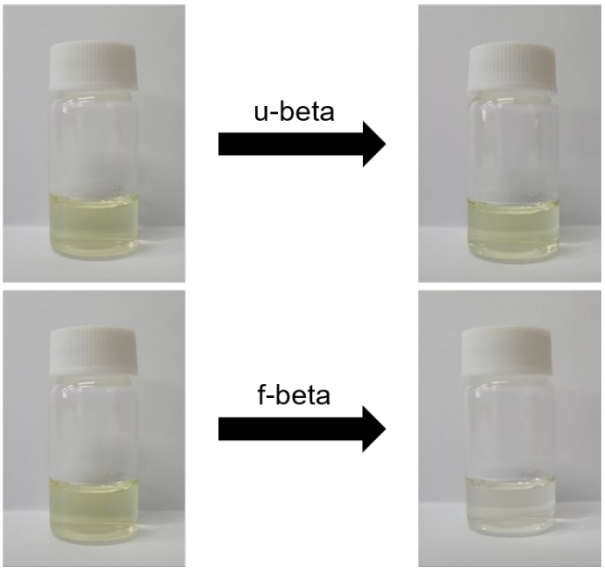

FigureS3. Photographs showing the color of the precursor solutions before (left) and after (right) continuous stirring with u-beta (top) and f-beta (bottom)

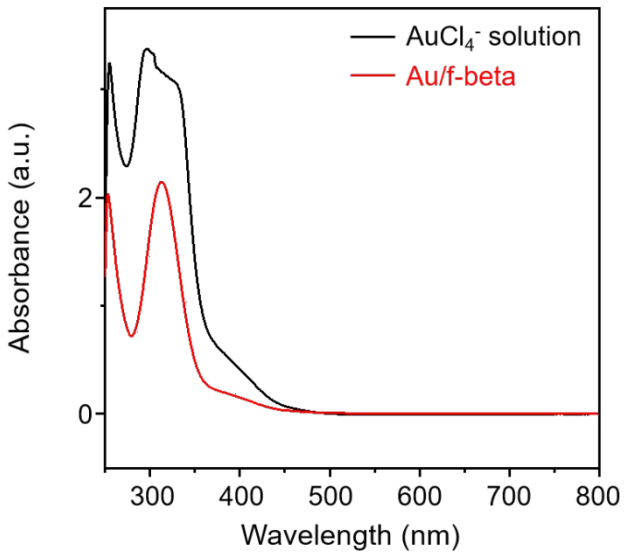

Figure S4. UV-visible spectra of a pure $AuCl_4^-$ solution (black line) and Au/f-beta filtrate (red line)

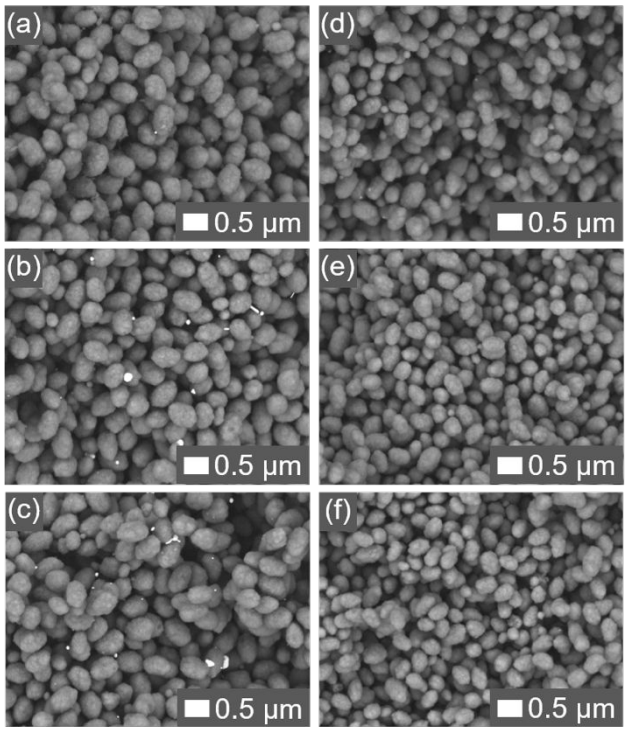

Figure S5. SEM images of Au/u-lab-beta (left-hand column) and Au/f-lab-beta (right-hand column) samples after $AuCl_4^-$ impregnation (a and d), O_2-calcination at 350 °C (b), O_2-calcination at 550 °C (e), and H_2-reduction at 350 °C (c and f)

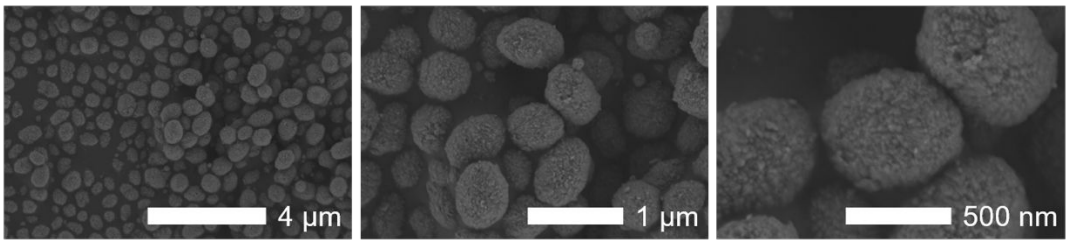

Figure S6. SEM images of zeolite beta prepared in the laboratory (i.e., u-lab-beta)

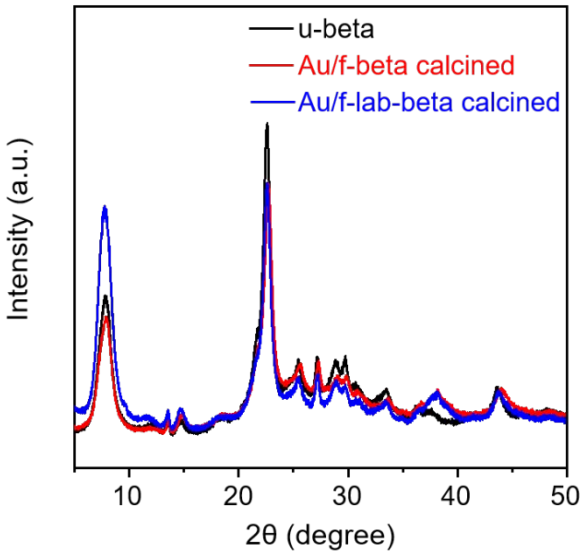

Figure S7. XRD patterns of Au/f-beta and Au/f-lab-beta samples after calcination; the XRD pattern of the commercial u-beta is displayed for comparison.

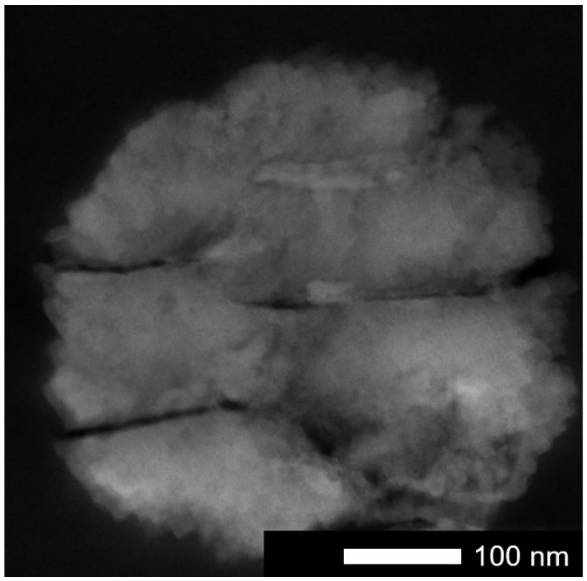

Figure S8. STEM image of the ultramicrotome-cross-sectioned Au/u-lab-beta sample after O_2 calcination at 350 °C

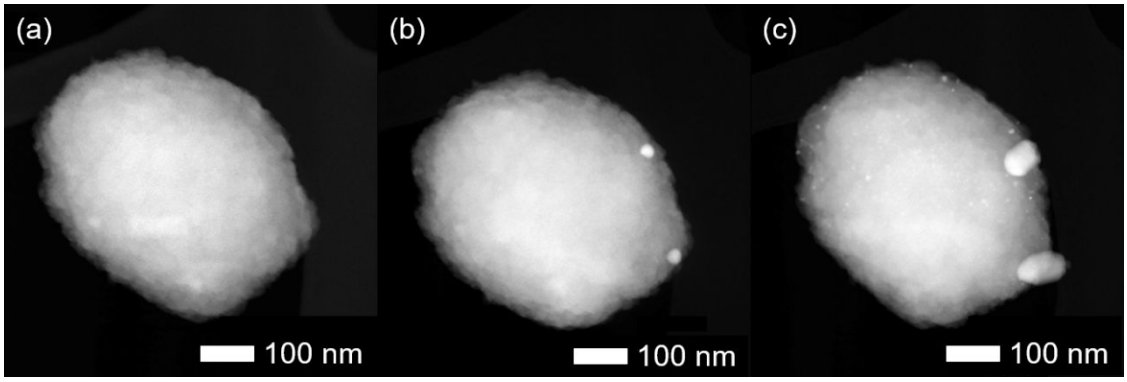

Figure S9. STEM images of in-situ heated Au/u-lab-beta as-synthesized (a), heated for 2 h at 550 °C (b), and the same crystal heated further for 2 h at 700 °C (c)

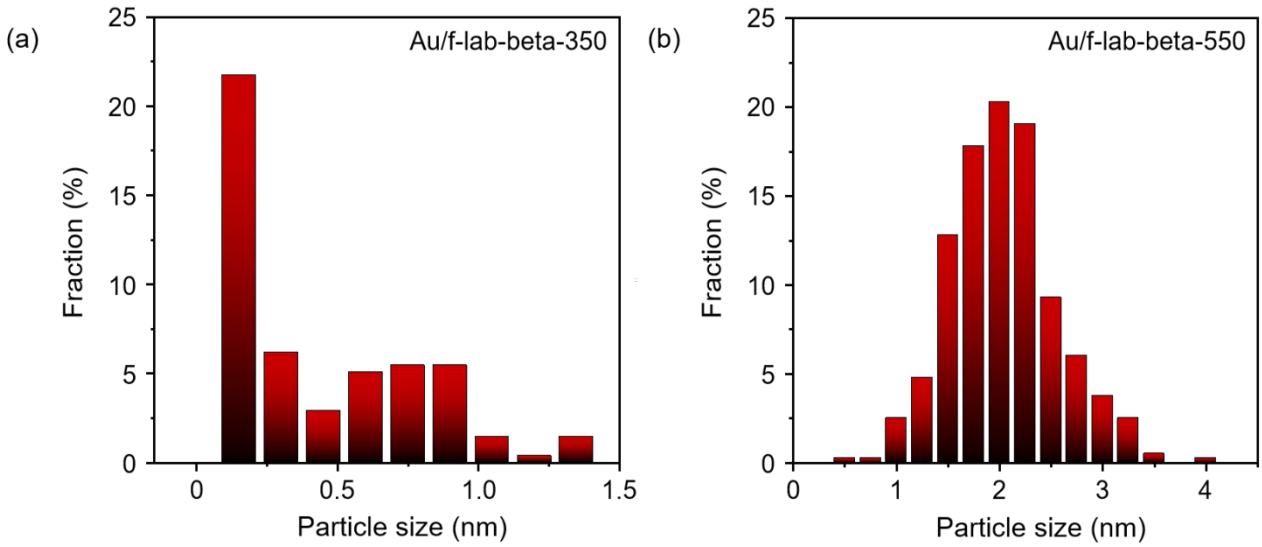

Figure S10. Particle size distributions of the Au metal supported on Au/f-lab-beta after calcination at (a) 350 °C and (b) 550 °C

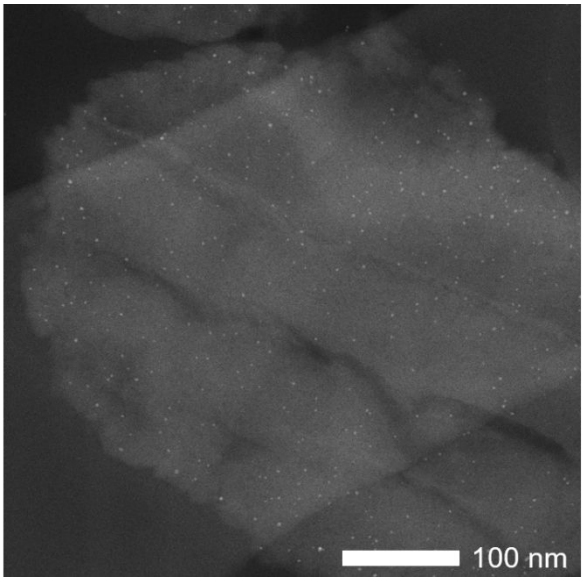

Figure S11. STEM image of the ultramicrotome cross-sectioned Au/f-lab-beta sample after O_2 calcination at 550 °C

(a)

Au/f-beta-350	
Nitrogen (%)	0.37
Carbon (%)	2.7
Hydrogen (%)	1.0
Sulphur (%)	0.49
Totals (%)	4.56

(b)

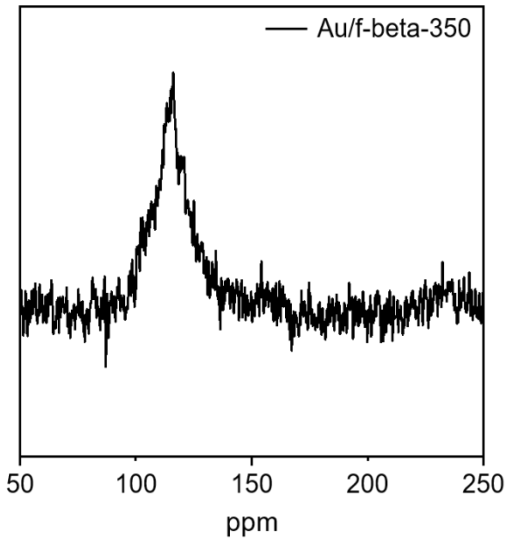

Figure S12. Elemental analysis (a), and $^{13}C\{^{1}H\}$ CP MAS NMR spectrum (b) of Au/f-beta after calcination at 300 °C

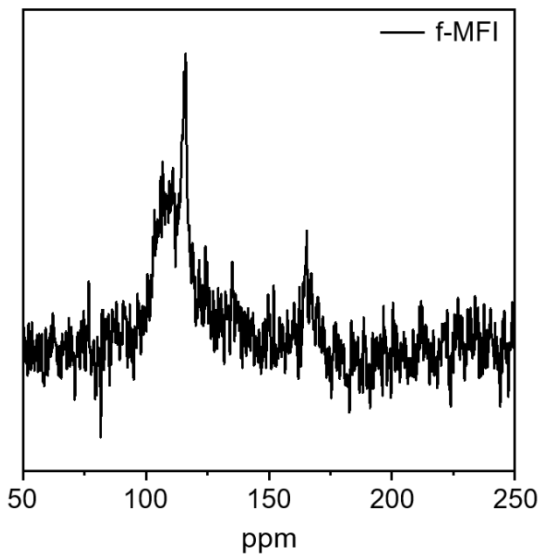

Figure S13. Solid-state $^{13}C\{^{1}H\}$ CP MAS NMR spectrum of f-MFI

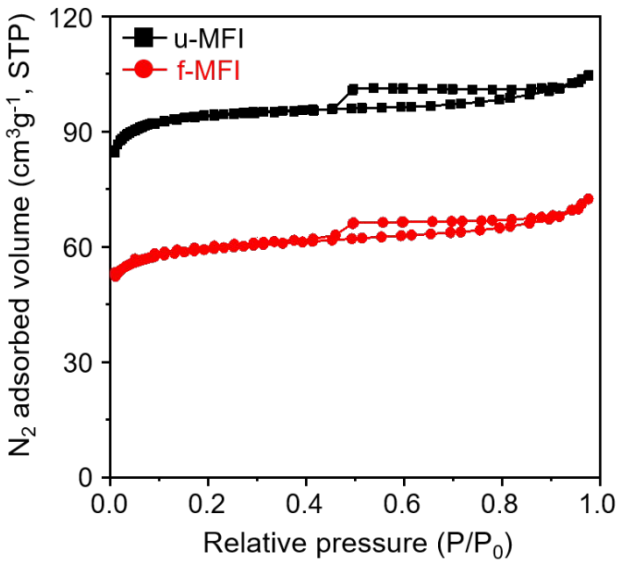

Figure S14. N_2 sorption isotherms of f-MFI and u-MFI samples

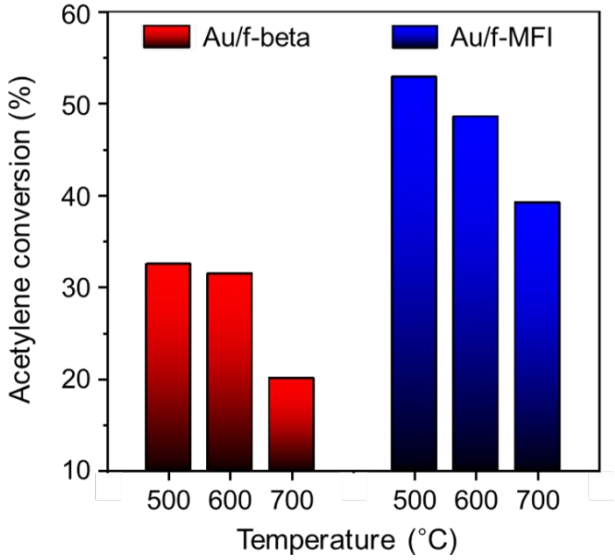

Figure S15. Mass activities of 0.48 Au/f-beta and 0.48 Au/f-MFI activated at various temperatures under the following reaction conditions: WHSV = 0.465 h^{-1}, temperature = 250 °C, mole ratio of C_2H_2: H_2: N_2 = 1: 10: 19

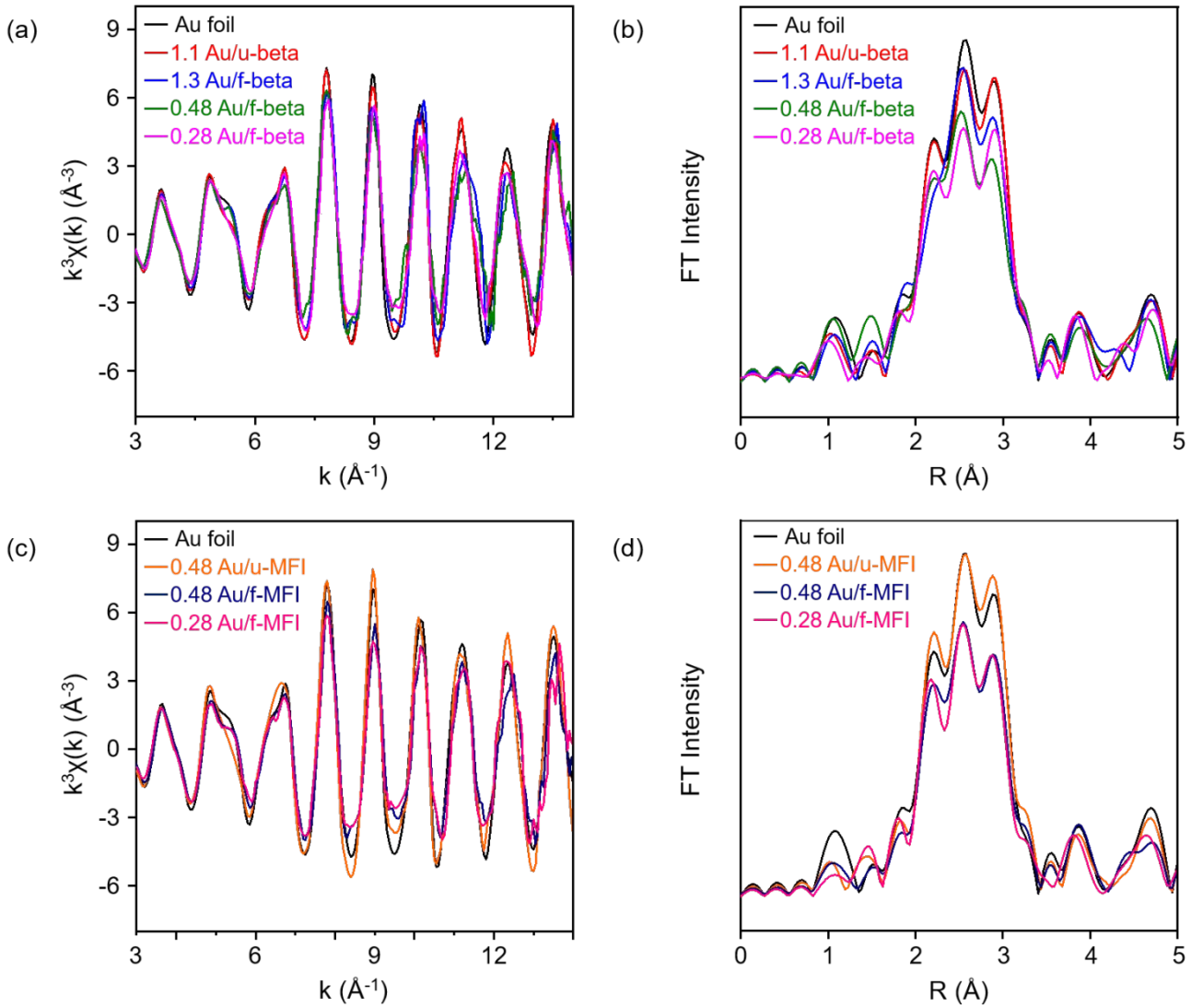

Figure S16. k $^3\chi(k)$ EXAFS spectrum (left-hand column) and the corresponding Fourier transforms (right-hand column) at Au L_3-edge of Au foil (black), 1.1 Au/u-beta (red), 1.3 Au/f-beta (blue), 0.48 Au/f-beta (green), 0.28 Au/f-beta (purple), 0.48 Au/u-MFI (orange), 0.48 Au/f-MFI (navy) and 0.28 Au/f-MFI (pink)

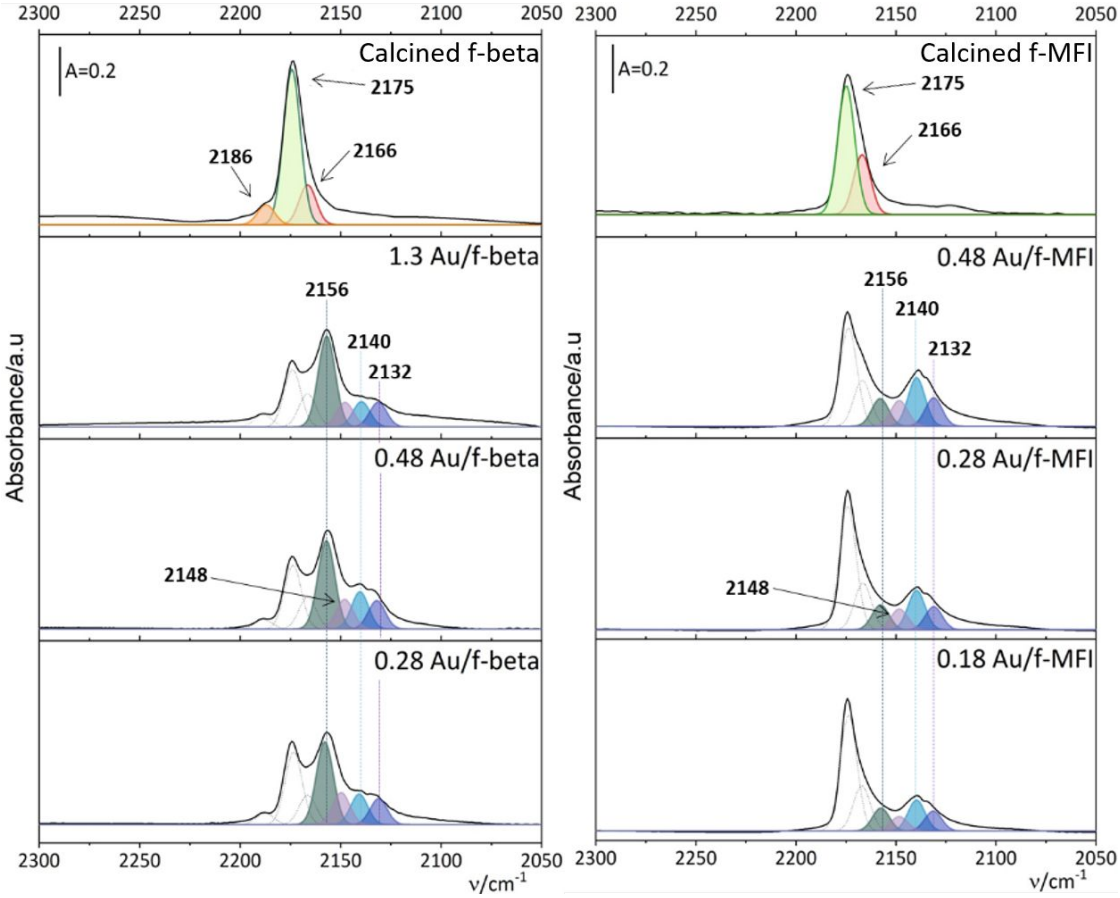

Figure S17. FTIR spectra of the calcined f-beta, 1.3 Au/f-beta, 0.48 Au/f-beta, 0.28 Au/f-beta, calcined f-MFI, 0.48 Au/f-MFI, 0.28 Au/f-MFI, and 0.18 Au/f-MFI recorded after exposure to CO until full saturation and subsequent removal of physically adsorbed CO at -150 °C.

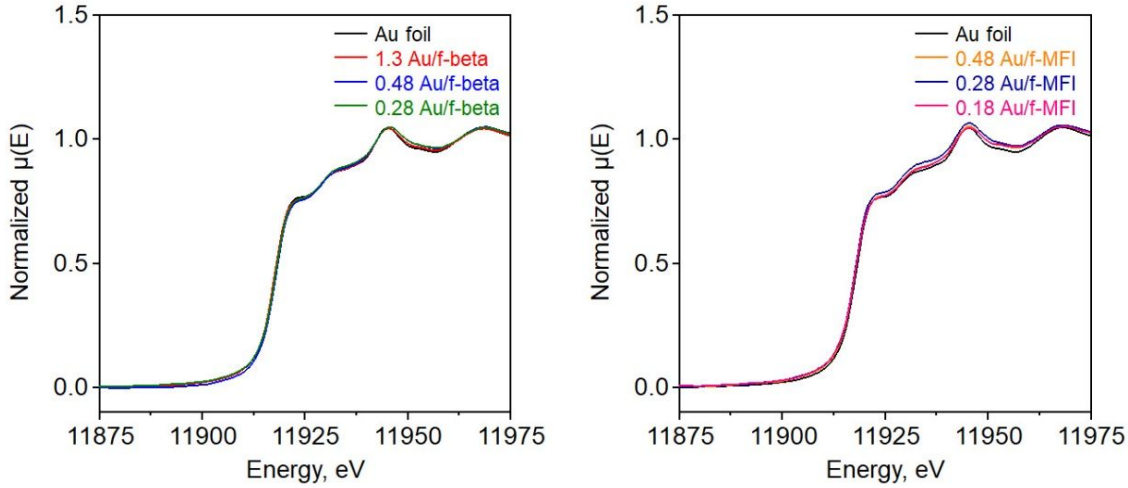

Figure S18. XANES spectra of Au foil, 1.3 Au/f-beta, 0.48 Au/f-beta, 0.28 Au/f-beta, 0.48 Au/f-MFI, 0.28 Au/f-MFI, and 0.18 Au/f-MFI, which was activated by H_2 reduction at 300 °C